Probing exciton density of states through phonon-assisted emission in GaN epilayers: *A* and *B* exciton contributions

Lucia Cavigli, Riccardo Gabrieli, and Massimo Gurioli
LENS, CNISM and Dipartimento di Fisica e Astronomia, Università di Firenze, Via G. Sansone 1, Sesto Fiorentino, I-50019 Florence, Italy

Franco Bogani
Dipartimento di Energetica, Università di Firenze, Via S. Marta 3, Firenze, I-50139 Florence, Italy

Eric Feltin, Jean-François Carlin, Raphaël Butté, and Nicolas Grandjean
Institute of Condensed Matter Physics, Ecole Polytechnique Fédérale de Lausanne, CH-1015 Lausanne, Switzerland

Anna Vinattieri*
CNISM, LENS and Dipartimento di Fisica e Astronomia, Università di Firenze, Via G. Sansone 1, Sesto Fiorentino, I-50019 Florence, Italy

(Received 12 April 2010; published 14 September 2010)

A detailed experimental investigation of the phonon-assisted emission in a high-quality *c*-plane GaN epilayer is presented up to 200 K. By performing photoluminescence and reflectivity measurements, we find important etaloning effects in the phonon-replica spectra, which have to be corrected before addressing the lineshape analysis. Direct experimental evidence for free exciton thermalization is found for the whole temperature range investigated. A close comparison with existing models for phonon replicas originating from a thermalized free exciton distribution shows that the simplified and commonly adopted description of the exciton-phonon interaction with a single excitonic band leads to a large discrepancy with experimental data. Only the consideration of the complex nature of the excitonic band in GaN, including *A* and *B* exciton contributions, allows accounting for the temperature dependence of the peak energy, intensity, and lineshape of the phonon replicas.

DOI: 10.1103/PhysRevB.82.115208 PACS number(s): 78.55.Cr, 71.35.−y, 71.38.−k

I. INTRODUCTION

Electron-phonon coupling is one of the fundamental interactions occurring in semiconductors, both bulk and nanostructures, which strongly affects their optical and electrical properties.[1,2] The electron dynamics is driven by the phonon emission, both optical and acoustic, and therefore the relaxation, thermalization and transport properties of charge carriers reflect these interactions. The same situation occurs when Coulombian interaction between electrons and holes gives rise to excitonic states. Different mechanisms (Fröhlich interaction, deformation and piezoelectric potentials) rule the electron-phonon interaction and important insights are commonly obtained by the study of the electron/exciton recombination dynamics.

If we focus on exciton recombinations, the exciton-phonon interaction determines the homogeneous thermal line broadening and therefore exciton dephasing mechanisms. A general rule is that the exciton-phonon interaction is larger in ionic II-VI semiconductors, with respect to the nearly covalent III-V compounds.[1] A remarkable effect of this difference can be found in the presence, in II-VI materials, of intense phonon replicas (PRs) of the excitonic emission, which are almost missing in GaAs and similar materials. At low cryogenic temperatures, excitonic recombinations in high quality ionic materials consist in the main radiative free exciton recombination lines [the so-called zero-phonon lines (ZPL)] and their PRs separated by an energy spacing close to $\hbar\omega_{LO}$ (the latter energy corresponding to the longitudinal optical phonon energy). The PR spectra not only contain information on the different mechanisms ruling the exciton-phonon interaction but they are also a useful tool for investigating the exciton recombination kinetics. The PR lineshape and intensity have been indeed the subject of thorough experimental and theoretical investigations in different semiconductor materials and nanostructures.[1–3]

Among III-V semiconductors, III-nitrides are unusual in so far as they exhibit a large ionic character and in fact PRs are a common feature of excitonic recombinations occurring in GaN-based systems.[2] Nitrides have been widely investigated in the last two decades for the development of several different kinds of light-emitting and high-power electronic devices.[4,5] Nevertheless, the poor optical quality of wurtzite III-nitride structures in terms of linewidth has hindered accessing for many years intrinsic effects. This is mainly due to strain inhomogeneities for heteroepitaxially grown bulk layers and to a large inhomogeneous broadening ascribed to composition fluctuations and internal electric fields for heterostructures grown along the *c* axis. Consequently, it made hard to extract reliable information on excitonic properties and, in particular, on the exciton-phonon interaction. Different models have been proposed to reproduce the PR features: initially a configurational model has been considered to extract the Huang-Rhys factor[6,7] from the ratio of the intensity of the replicas which arise from the radiative recombination of excitons assisted by the emission of *n* phonons. The analysis of PRs originating from strongly localized excitons or excitons bound to defects was satisfactorily interpreted in the framework of this model.[8–10] Recently, the quality of nonintentionally doped (nid) wurtzite GaN epilayers has been

greatly improved and the free exciton recombination can prevail over the bound exciton recombination even at low temperature. Clear features arising from the *A* and *B* exciton recombinations have been reported in the ZPL photoluminescence (ZPL-PL) of GaN epilayers[11,12] and even in quantum wells.[13,14] This has made possible the comparison with models where the intrinsic nature of the exciton is considered. Detailed investigations have been already reported concerning the phonon-induced thermal broadening of the excitonic lines and the main characteristics of the phonon-assisted emission.[15] Until now, experimental studies dealing with the spectral shift,[16–20] intensity,[21–23] and lineshape[12,17,19,20,22–25] of PR emission with temperature (T) have been performed in a restricted T range ($T<100$ K) and subsequent modeling of the data systematically neglected the *B* exciton contribution. A careful analysis of the reported data, mainly those measured at higher T concerning the PR spectral shift[16,20] and lineshape,[16,17,19,20,23,25] evidences only a poor agreement with the model predictions. Only few studies analyzed the spectral lineshape, ascribing discrepancies with the model to the presence of residual impurity scattering.[25]

In this paper we present experimental results in an extended T range (10–200 K), on the ZPL and PR luminescence of a high-quality nid GaN epilayer grown on a *c*-plane sapphire substrate. A crossed analysis between photoluminescence and reflectivity (R) experiments, performed by collecting both signals from the same spot on the sample, allows us to assess the exciton thermalization in the ZPL and PR bands and to compare the 1LO- and 2LO-phonon emissions with the model commonly accepted[26,27] in the whole T range investigated. We clearly show that to fully describe the experimental results, both the *A* and *B* excitonic bands have to be taken into account. In this way we demonstrate a very satisfactory agreement with the theoretical model when the complexity of the GaN valence band is considered.

II. THEORETICAL CONSIDERATIONS

The established theory[26,27] describes the nth PR intensity $I_n(E)$ and its lineshape in terms of the Fröhlich interaction between excitons and LO-phonons. Under the assumption of a quasithermal exciton distribution, the intensity of the nth phonon replica turns out to be given by

$$I_n(E_X+E_k-n\hbar\omega_{\mathrm{LO}}) \approx \mathrm{W}_n(E_k)\rho(E_k)e^{-E_k/k_BT}, \qquad (1)$$

where E_X is the ZPL transition energy, E_k is the exciton center of mass kinetic energy, $\rho(E_k)$ indicates the exciton density of states (DOS), $\mathrm{W}_n(E_k)$ is the energy-dependent probability that an exciton with kinetic energy E_k recombines emitting n phonons and T is the effective excitonic temperature. In the framework of a perturbative approach to describe the exciton-phonon interaction, W_n depends linearly on the energy E_k for odd replicas whereas it is energy independent for even replicas, as a consequence of energy and momentum conservation.[26,27] The emission probability in Eq. (1) is weighted by the Boltzmann factor which accounts for a thermalized nondegenerate exciton distribution. If we consider an ideal bulk sample we should therefore expect that different PRs have distinctive features related to the density of states and the matrix element. In particular, for a single free exciton band in an isotropic three-dimensional system (i.e., assuming $\rho(E_k)\propto\sqrt{E_k}$), the energy $E_{1\mathrm{LO}}(T)$ $[E_{2\mathrm{LO}}(T)]$ corresponding to the maximum of the first (second) phonon replica depends linearly on T with a characteristic slope[26,27]

$$E_{1\mathrm{LO}}(T) = E_X(T) - \hbar\omega_{\mathrm{LO}} + 1.5k_BT, \qquad (2)$$

$$E_{2\mathrm{LO}}(T) = E_X(T) - 2\hbar\omega_{\mathrm{LO}} + 0.5k_BT, \qquad (3)$$

where $E_X(T)$ includes the band gap shrinking. Moreover, different spectral shapes are expected for the 1LO and 2LO-phonon emission and, concerning the ratio of the spectrally integrated intensities $I_{1\mathrm{LO}}/I_{2\mathrm{LO}}$ a linear dependence on k_BT is expected.

III. EXPERIMENTAL DETAILS

The investigated sample is a 3 μm thick nid wurtzite GaN epilayer grown by metal organic vapor phase epitaxy (MOVPE) on a *c*-plane sapphire substrate characterized by a threading dislocation density lower than 1×10^9 cm^{-2}. All measurements were performed with the sample placed in a closed-cycle cryostat in the temperature range 10–200 K. R measurements at normal incidence were carried out using a CW Xe lamp. The light was spatially filtered in order to obtain a spot size on the order of 0.5 mm. Time-integrated photoluminescence (TI-PL) measurements were performed under nonresonant excitation by a frequency-doubled dye laser, providing 8 ps pulses at 300 nm with a repetition rate of 76 MHz using a laser spot size matched to that of the white light spot issued from the Xe lamp. R and PL experiments probed the same sample region to ensure a careful and systematic analysis of the band-edge properties. In both cases, the collected light was detected by a cooled silicon charge coupled device camera after dispersion through a 50-cm-flat field spectrometer offering a spectral resolution of 0.5 meV.

IV. DISCUSSION

In Fig. 1, a typical PL spectrum is shown at 10 K for (a) the ZPL spectral range and for (b) the PR region. The main spectral features observed in the ZPL region at 10 K are related to the neutral donor-bound exciton recombination ($\mathrm{D}^0\mathrm{X}_A$) and to the X_A and X_B exciton radiative recombinations. The emission from the 2S state of X_A excitons is also detected at higher energy. Fitting the ZPL with a Gaussian lineshape allows to extract an inhomogeneous broadening of the X_A emission band with a full width at half maximum (FWHM) of 3 meV, indicating the high quality of this MOVPE-grown epilayer and its excellent strain homogeneity, corresponding to a biaxial stress variation in ±1.0 kbar.[28] The reflectivity spectrum (gray line in Fig. 1) shows clear excitonic resonances confirming the attribution of the PL structures: a very small Stokes shift (≈1 meV) is detected, which disappears at higher temperature, indicating a minor contribution from localized excitons. The energy separation between the excitonic resonances X_B and X_A, derived from the reflectivity spectra, is $E_{\mathrm{X}_B}-E_{\mathrm{X}_A}=8.0\pm0.5$ meV, in agreement with values reported in the

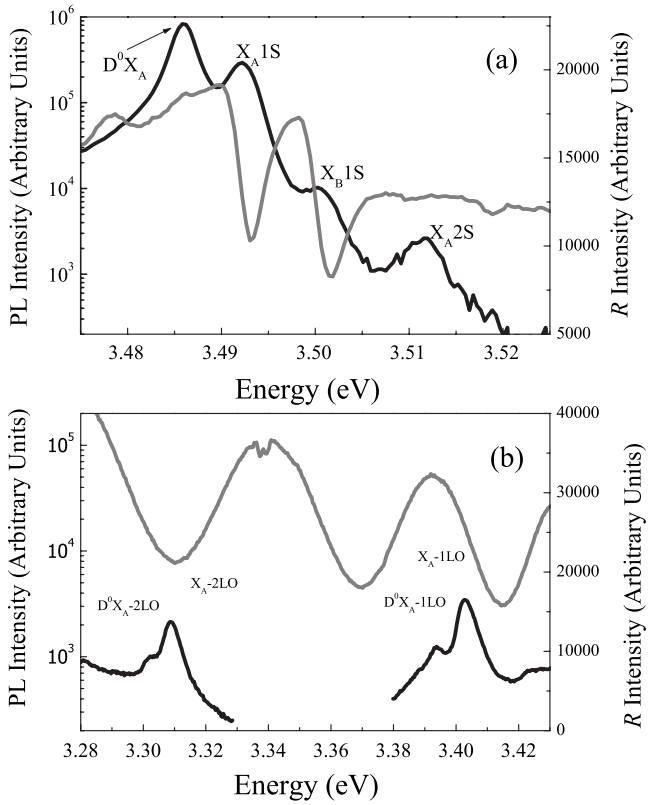

FIG. 1. PL (black line, semilog scale) and reflectivity (gray line, linear scale) spectra measured at 10 K in the (a) ZPL and (b) PR regions, respectively.

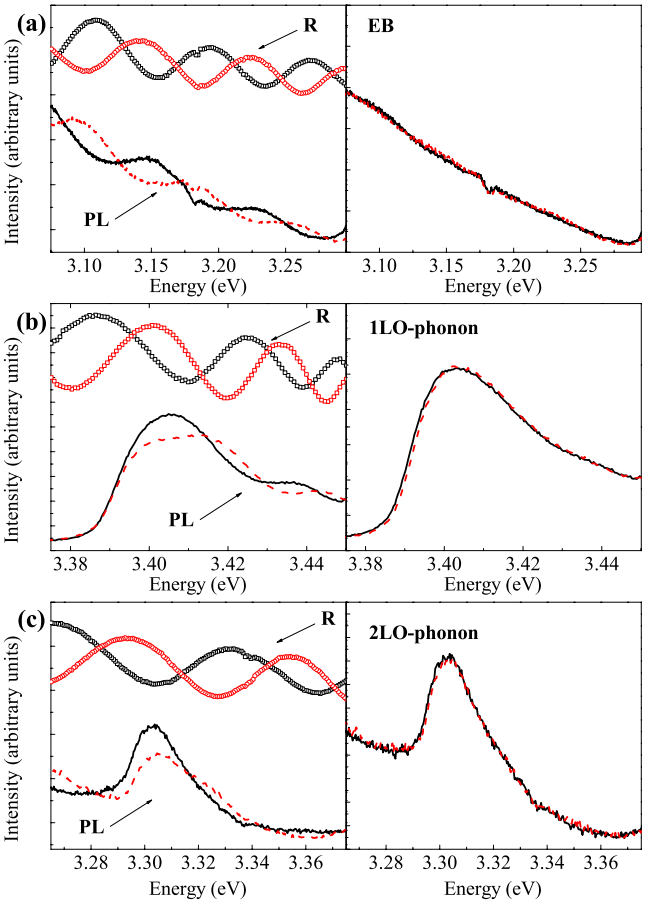

FIG. 2. (Color online) On the left-hand side two PL spectra measured at $T=140$ K, detected at two different points on the sample and their corresponding reflectivity spectra (open symbols) are compared. On the right hand side, the PL spectra are displayed after correction with Eq. (4): (a) in the EB region, (b) in the 1LO-phonon region, and (c) in the 2LO-phonon region. A given color refers to a given position on the sample.

literature for GaN epilayers grown on *c*-plane sapphire.[11] Phonon-replicas of D ^0X_A and X_A states measured at 10 K are observed for the first and second order [Fig. 1(b)]. An energy separation of $\hbar\omega_{LO}=92\pm0.5$ meV is measured between the D ^0X_A state and its 1LO-phonon replica, in agreement with Raman spectroscopy and inelastic x-ray scattering results.[29–31] At this stage, it is worth noticing that at 10 K in the PR spectral region reflectivity spectra exhibit a modulation with a period much larger than the FWHM of the PR lines.

When increasing the temperature we observe an unexpected structuring of the replica lineshapes as reported in the left hand side of Figs. 2(b) and 2(c), where data measured at $T=140$ K are reported. Different PR lineshapes are found for different points in the sample, denoting a spatially dependent nature of the PR structuring while the ZPL lineshape (not reported here) does not change when probing different spatial regions of the sample. Note that even the energy of the maximum of the PR band is position dependent. This implies that any direct comparison of PR-PL data with the current theoretical model,[26,27] concerning either the peak position or the lineshape cannot be based on measured spectra, as usually done in the literature.

The comparison of PL spectra with corresponding reflectivity spectra, reported as open symbols in the left hand side of Fig. 2, clarifies the nature of the extrinsic PR lineshape. The appearance of structures in the replicas, as the thermal broadening gets important, is an artifact related to an interference effect as clearly shown by the reflectivity spectra. In the spectral region where very weak absorption is present, we observe a strong modulation both in the reflectivity and PL signals. On the basis of the coincidence of the modulation spacing observed in both R and PL spectra we conclude that the PR modulation comes from a pure etaloning effect. It is worth noting that this etaloning effect shows a phase shift strongly dependent on the point probed on the sample, possibly due to a wedge in the epitaxially-grown sample originating from the miscut angle of the substrate. Therefore, on one side this etaloning effect can be used for detecting details of the sample growth and, on the other hand and on a more relevant aspect for the content of this paper, PL spectra have to be appropriately corrected for multiple interference effects. Given the energy scale of the interference pattern, the modification of the PR lineshape gets more important as $T\geq80$ K, when the PR band becomes broad. Hence an appropriate correction is required before comparing the experimental PR lineshape and PR energy peak position with the model[26,27] in the high-temperature range ($T\geq80$ K).

In principle, etaloning could be avoided by choosing a thick sample, as done, e.g., in Ref. 12 by using freestanding hydride vapor phase epitaxy grown GaN layers. Our choice

to work on thin GaN epilayers grown on a *c*-plane sapphire substrate relies, however, on several important motivations: (i) III-nitride based light-emitting diodes are still mostly grown on *c*-plane sapphire substrates and most of the research work carried out in academic institutions is performed on samples grown on such a substrate; (ii) the present work will point out a generalized misunderstanding regarding GaN epilayers grown on *c*-plane sapphire substrates, namely, the weight of the intrinsic exciton-phonon interaction deduced from experiments systematically entails errors which prevent an accurate comparison with the commonly adopted models described in Refs. 26 and 27.

Interference effects have been already reported for III-nitride heterostructures and the corresponding PL spectra have been corrected on the basis of specific models.[32,33] In our case, to account for this effect and correct accordingly the PR lineshape, we consider that the sample acts as a spectral filter for the luminescence below the energy bandgap. Therefore we consider a transfer function $TF(E)$ between the internal PL and the external (measured) PL. Since in the spectral region of interest the absorption is negligible, $TF(E)$ is proportional to the transmittivity $T(E)$ $[TF(E) \propto T(E) = 1 - R(E)$, $R(E)$ being the reflectivity]. In the absence of an absolute value of the reflectivity we can correct the PL intensity using the following phenomenological expression:

$$I_{\mathrm{PL}}^{Corr}(E) = \frac{I_{\mathrm{PL}}(E)}{TF(E)} = \frac{I_{\mathrm{PL}}(E)}{1 - \gamma R^{Exp}(E)}, \tag{4}$$

where $R^{Exp}(E)$ is the experimental reflectance spectrum detected from the same spot than the PL one and γ is a constant fitting parameter $[R(E) = \gamma R^{Exp}(E)]$. If we assume that the extrinsic extended band (EB) below 3.2 eV (Refs. 8 and 34) has a structureless shape and that its modulation is due to an etaloning effect, γ is fixed by imposing the cancellation of the etaloning in the same band.

PL spectra corrected using Eq. (4) are reported in the right hand side of Fig. 2. The modulation is canceled not only for the EB band but also and quite effectively for the first and second PR bands. As a consequence the corrected PR spectra [right hand side of Figs. 2(b) and 2(c)] exhibit the same structureless lineshape, independently of the probed spatial region. The reconstruction of an intrinsic lineshape for the PR spectra allows us to perform an accurate study of their lineshape in a wider temperature range, as compared with previous studies. Hereafter the reported PR spectra will refer to spectra after the etaloning correction.

In Fig. 3 we show the PL lineshape at different temperatures, normalized to the X_A emission and shifted so as to align the energy position of the X_A exciton. The ZPL band [Fig. 3(a)] shows a quenching of the D ^0X_A recombination, the thermal population of the X_B exciton and a clear exponential tail, in the high-energy side, coming from free carrier recombination. The huge thermal tail eventually masks the X_C exciton contribution, even though at 160 K a change in the slope 30 meV above the X_A emission is observed. Concerning the PR lineshape [Figs. 3(b) and 3(c)] the first two replicas exhibit a significant thermal broadening and a blueshift of the emission with respect to the ZPL, as expected from the model proposed for the phonon replica emission

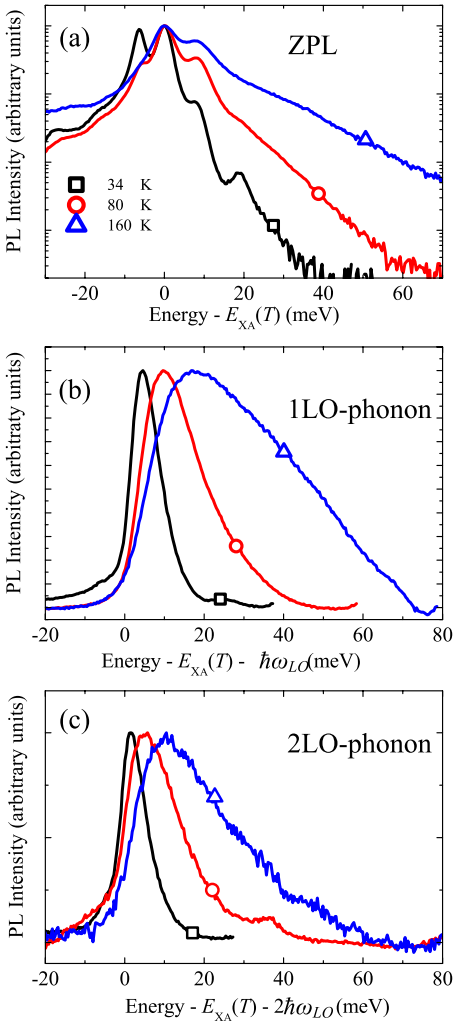

FIG. 3. (Color online) PL spectra for three different temperatures (black line, open square $T=34$ K, red line, open circle $T=80$ K, blue line, open triangle $T=160$ K), (a) in the ZPL region, normalized to the X_A intensity and setting as energy zero the energy of X_A; (b) in the 1LO-phonon region, normalized to the X_A intensity and subtracting to the energy scale the value of the X_A energy and the LO-phonon energy $\hbar\omega_{\mathrm{LO}}=92$ meV; (c) in the 2LO-phonon region, normalized to the X_A intensity and subtracting to the energy scale the value of the X_A energy and twice the LO-phonon energy $\hbar\omega_{\mathrm{LO}}$.

from a thermalized distribution of free excitons.

In order to assess the validity of Eq. (1),[26,27] the starting point is to confirm the presence of a quasithermalized exciton distribution. Under this assumption, the ZPL intensity is given by

$$I_{\mathrm{ZPL}}(E) \approx \alpha(E)\exp\left[-\frac{E}{k_B T_{\mathrm{eff}}}\right], \tag{5}$$

where $\alpha(E)$ is the absorption coefficient and T_{eff} is the effective temperature of the exciton distribution, which can be eventually different from the nominal lattice temperature T_L, as already demonstrated in III-V nanostructures.[35] Since a lack of thermalization might be present at low lattice temperatures, we assume $T_{\mathrm{eff}}=T_L$ for $T_L > 50$ K and we extract

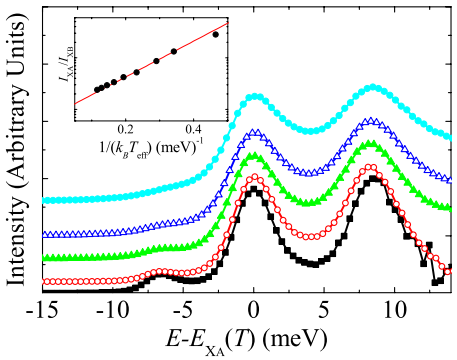

FIG. 4. (Color online) Ratio of the PL intensity and Boltzmann factor at different temperatures: full squares $T=27$ K, open circles $T=34$ K, full triangles $T=50$ K, open triangles $T=70$ K, full circles $T=100$ K. Inset: ratio of the spectrally integrated intensity of X_A/X_B excitons in semilog scale as a function of the inverse of temperature. The solid line is a fit to the data with the expression $\exp(\Delta E/k_BT)$.

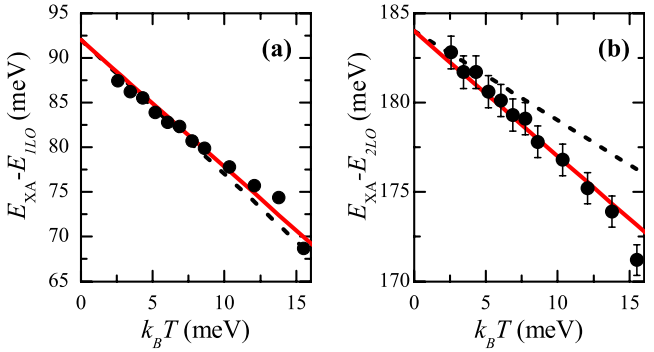

FIG. 5. (Color online) (a) Energy separation X_A-1LO as a function of k_BT. (b) Energy separation X_A-2LO as a function of k_BT. Solid lines are linear fits to the data. Dashed lines correspond to the k_BT dependence expected from Eq. (1) considering only the A exciton band contribution.

from Eq. (5) the absorptionlike profile dividing $I_{ZPL}(E)$ by the Boltzmann factor. These profiles are reported in Fig. 4 for several temperatures as a function of the energy difference with respect to the energy position of the A free exciton E_{X_A}. It is clear that they show almost identical lineshapes denoting the validity of the exciton thermalization hypothesis. In order to obtain the same profile when $T_L<40$ K, we have to assume for the exciton population a higher temperature T_{eff} with respect to the lattice one, indicating that exciton thermalization occurs even at $T_L<40$ K but the thermal equilibrium occurs at a slightly higher temperature. In particular for $T_L=10$ K we found $T_{\text{eff}}=27$ K.[36]

The absorptionlike profiles show two nice excitonic resonances separated by 8 meV in agreement with the X_B-X_A energy separation observed in the reflectivity spectrum. Another proof of the existence of a thermalized exciton distribution, over both the A and B bands, is given by the ratio of the spectrally integrated intensity from the X_A/X_B excitons. This is reported in a semilogarithmic scale as a function of $1/k_BT_{\text{eff}}$ in the inset of Fig. 4, where the solid line is a fit to the data with $\exp(\Delta E/k_BT)$ and we found $\Delta E=8.0\pm0.5$ meV, which nicely agrees with the X_B-X_A energy separation. In the following we will therefore indicate the thermal energy k_BT as the "effective" thermal energy k_BT_{eff}, as deduced from the absorptionlike spectra of Fig. 4.

Having proved the validity of the exciton thermalization hypothesis and established the corrected temperature to be used, at least as long as a time-integrated emission is considered, let us start with the analysis of the energy position of the PL bands, denoted as $E_{1LO}(T)$ for the first PR and $E_{2LO}(T)$ for the second PR. In Figs. 5(a) and 5(b) we report the energy separation $E_{X_A}(T)-E_{1LO}(T)$ and $E_{X_A}(T)-E_{2LO}(T)$, respectively, as a function of k_BT: a linear dependence is found in both cases as expected from Eqs. (2) and (3). We performed a linear fit by assuming the LO-phonon energy $\hbar\omega_{LO}=92$ meV as experimentally measured in our sample from the D ^0X_A phonon replica at low temperature. For the first PR the best fit gives a slope of -1.4 ± 0.1, close to the theoretical prediction of -1.5, both of them being displayed as solid and dashed lines, respectively, in Fig. 5(a). For the second PR, instead, the energy shift is significantly different from the established model. In fact we find a slope of -0.70 ± 0.05, against an expected value of -0.5. The best fit and the theoretical prediction of Eq. (1), with only the A band, are reported as solid and dashed lines, respectively, in Fig. 5(b). Clearly experimental data are largely off the theoretical predictions.

It is important to note that if the etaloning correction is not performed, the $E_{X_A}-E_{1LO}$ and $E_{X_A}-E_{2LO}$ exhibit a linear dependence on the temperature with the same slope as observed in Fig. 5 but with an intercept, at $T=0$ K, different from the LO phonon energy. In particular, for the 2LO, the intercept is 2 meV higher than $\hbar\omega_{LO}$. Then the etaloning correction has mainly the effect of recovering the correct LO phonon energy without affecting the slope.

In order to get more insights into the origin of the observed deviation from the established theory, we display in Fig. 6 the calculated quantity ρW_n, as obtained from experimental spectra divided by the Boltzmann factor after background subtraction and etaloning correction for three different temperatures. The zero of the energy scale corresponds to the onset of the replica at the energy $E_{X_A}-n\hbar\omega_{LO}$. These profiles, according to Eq. (1),[26,27] should lead to the function $\rho(E_k)W_n(E_k)$. Experimental data measured at different temperatures show very similar profiles, even if they extend over a different energy range for different values of T, given the limited dynamic range in the data. This is a further confirmation of the validity of the exciton thermalization hypothesis and, at the same time, it demonstrates that direct information on the intrinsic exciton-phonon interaction can be obtained from the analysis of the PR lineshapes. Accordingly to theoretical models[26,27] $\rho(E_k)\propto\sqrt{E_k}$, $W_1(E_k)\propto E_k$, and $W_2(E_k)$ is energy independent, so in a single-band model we should find $\rho(E_k)W_1(E_k)\approx E_k^{1.5}$ and $\rho(E_k)W_2(E_k)\approx E_k^{0.5}$. These two functions are reported as light-blue dashed-dotted lines in Fig. 6. While, for the 1LO-phonon replica, the single band model reproduces quite well the experimental values, a large discrepancy is found for the 2LO-phonon replica, which has to reproduce the exciton DOS, as long as $W_2(E_k)$ is energy independent. We then fit the data using a power law

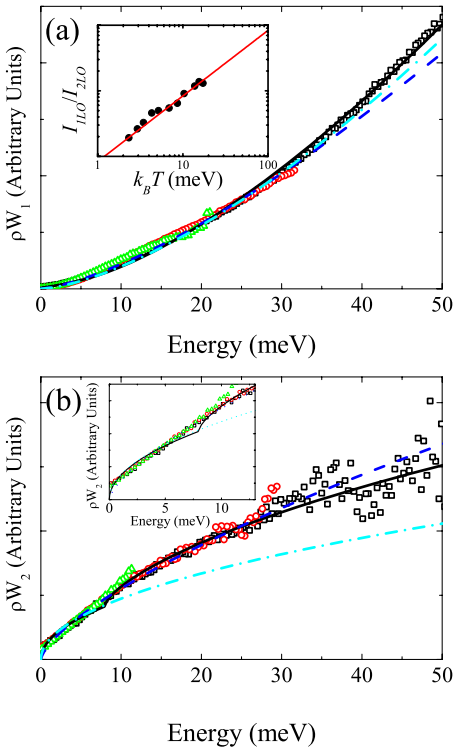

FIG. 6. (Color online) The calculated quantity ρW_n, as obtained from experimental spectra divided by the Boltzmann factor, after background subtraction and etaloning correction for three different temperatures (open green triangles $T=34$ K, open red circles $T=80$ K, open black squares $T=160$ K) (a) from 1LO-phonon TI-PL spectra. Inset: ratio of the spectrally integrated emission of the 1LO- and 2LO-phonon replica intensity as a function of k_BT. The solid line is a fit to the data with a power law $A(k_BT)^{\beta}$; and (b) from 2LO-phonon TI-PL spectra. Light blue dashed-dotted lines are the power laws expected from Eq. (1). Blue dashed lines are fits to the data according to a power law with the α exponent kept as a free parameter (see text for details). Black solid lines are fits to the data following Eq. (6). Inset: close-up view showing the discontinuity due to the contribution of the B exciton.

E^{α} with the exponent α kept as a free parameter (blue dashed lines in Fig. 6). It turns out that the best fit exponents are 1.4 ± 0.1 for the first replica and 0.7 ± 0.1 for the second replica, which nicely agrees with the coefficients found in Fig. 5. Therefore the discrepancy between our data and the commonly accepted picture for PRs in GaN is further confirmed.

Generally speaking this discrepancy may arise from an incorrect evaluation either of the exciton DOS $\rho(E_k)$, due to nonparabolicity effects or to the degeneracy of the excitonic band,[37–40] or to the exciton-phonon interaction $W_n(E_k)$. An interesting clue on this puzzling scenario can be found in the analysis of the spectrally integrated intensity of the first I_{1LO} and second I_{2LO} PR spectra. The ratio I_{1LO}/I_{2LO} is independent of the details of the excitonic density of states (which is the same for the two PL bands) and gives information on the exciton-phonon interaction. Integrating Eq. (1) and assuming $W_n(E_k)\propto(E_k)^{\alpha_n}$, we find $I_{1LO}/I_{2LO}\propto(k_BT)^{\beta}$ with $\beta=\alpha_1-\alpha_2$ regardless of the profile of the excitonic DOS; as stated previously, the theoretical prediction is $\beta=1$. Experimental data for I_{1LO}/I_{2LO} are reported as a function of k_BT in the inset of Fig. 6(a) and the best fit to the data with a power law $I_{1LO}/I_{2LO}=A(k_BT)^{\beta}$ gives $\beta=1\pm0.05$. Therefore as experimental data are in good agreement with the theoretical predictions for $W_n(E_k)$, we conclude that the previously discussed discrepancy between data and theory is likely due to an incorrect estimation of the exciton DOS $\rho(E_k)$.

A very simple correction to the excitonic density of states $\rho(E_k)\propto\sqrt{E_k}$ is related to the presence of different excitonic states in the wurtzite GaN system. The C exciton can be neglected in the T range considered here but, as shown in Fig. 3(a), the B exciton band becomes significantly populated as the temperature is greater than a few tens of Kelvin. Such population will also play a role in the phonon-assisted emission, even though no clear band structuring is observed at high temperature in the PRs, besides the etaloning effects. By considering the presence of the B excitonic band, the theoretical function to be compared with the data in Figs. 6(a) and 6(b), is

$$\rho(E_k)W_n(E_k)=A_n[(E_k)^{\alpha_n+(1/2)}+c_n(E_k-E_{X_B})^{\alpha_n+(1/2)}], \tag{6}$$

where $\alpha_1=1$ and $\alpha_2=0$. The factor c_2 accounts for the different exciton masses in the A and B bands. Neglecting a possible different Fröhlich interaction in the 1LO-phonon replica for the A and B excitons,[27] we set $c_1=c_2$. From the values reported in the literature[12] $c_{1(2)}$ has been fixed to 0.5. In order to fit the experimental data of Fig. 5 with Eq. (6) the only parameter is A_n, all other quantities being experimentally determined. The black solid lines of Figs. 6(a) and 6(b) are fits to the data according to Eq. (6), evidencing a nice agreement between experimental results and theoretical predictions. Note that no excitonic broadening has been introduced in those fits. Despite this crude approximation only a slight discontinuity in the theoretical profile of the second PR is observed at the onset of the B exciton density of states, which can be washed out by considering excitonic broadening. This also explains the absence of spectral structuring, related to the B exciton, in the phonon replica emission (Figs. 1 and 2). It is also worth stressing that the energy-dependent exciton-phonon interaction strongly reduces the relative weight of the B exciton in the first replica, explaining the better agreement between experimental data and single-band theory in this case. As shown, the presence of the exciton B contribution in the DOS completely accounts for the apparent discrepancy discussed above. The comparison of the black solid lines and the dark blue dashed lines in Figs. 6(a) and 6(b) evidences that the exciton DOS including the A and B contribution results in an effective DOS $\rho_{eff}(E_k)\propto(E_k)^{0.7}$, which gives the observed slope for the 2LO-phonon replica shift.

Moreover the very satisfactory agreement of the experimental data with the two-band model (black solid lines in Fig. 6) implies a full reconstruction of PR lineshapes in the whole investigated T range.

V. CONCLUSIONS

We have presented a detailed experimental investigation of the phonon replica emission in a high-quality c-plane GaN

epilayer grown on sapphire. We have proved that care has to be taken when analyzing PR spectra, due to the presence of multiple interference effects. The simultaneous measurement of PL and R spectra allows us to correct for etaloning effects and to reconstruct the intrinsic PR lineshapes. Direct evidence for exciton thermalization is found by the analysis of the ZPL and the PR bands in all the investigated temperature range. In addition we demonstrated that the excitonic temperature is larger than the nominal lattice temperature in the low T range. The comparison with existing models to describe the PR lineshape and intensity shows that the complex nature of the exciton band in GaN has to be considered to fully account for the PR energy-shift, lineshape, and intensity.

We believe that our results represent an important step forward to the understanding of intrinsic excitonic features in GaN-based structures. In particular, the issues of exciton thermalization and phonon driven exciton relaxation are of outmost relevance for nitride microcavities.

ACKNOWLEDGMENTS

This work was supported by the NCCR Quantum Photonics, research instrument of the Swiss National Science Foundation, by the Grant No. 200020-113542.

*vinattieri@fi.infn.it

[1] C. F. Klingshirn, *Semiconductor Optics*, 3rd ed. (Springer-Verlag, Berlin, 2007).
[2] B. Gil, *Low-Dimensional Nitride Semiconductors* (Oxford University Press, New York, 2002).
[3] F. Rossi and T. Kuhn, Rev. Mod. Phys. **74**, 895 (2002).
[4] S. Nakamura, G. Fasol, and S. J. Pearton, *The Blue Laser Diode: The Complete Story* (Springer-Verlag, Berlin, 2000).
[5] Y. Narukawa, Y. Kawakami, M. Funato, S. Fujita, S. Fujita, and S. Nakamura, Appl. Phys. Lett. **70**, 981 (1997).
[6] K. Huang and A. Rhys, Proc. R. Soc. London, Ser. A **204**, 406 (1950).
[7] M. Smith, J. Y. Lin, H. X. Jiang, A. Khan, Q. Chen, A. Salvador, A. Botchkarev, W. Kim, and H. Morkoc, Appl. Phys. Lett. **70**, 2882 (1997).
[8] M. Leroux, N. Grandjean, B. Beaumont, G. Nataf, F. Semond, J. Massies, and P. Gibart, J. Appl. Phys. **86**, 3721 (1999).
[9] S. Kalliakos, P. Lefebvre, X. Zhang, T. Taliercio, B. Gil, N. Grandjean, B. Damilano, and J. Massies, Phys. Status Solidi A **190**, 149 (2002).
[10] S. Kalliakos, X. B. Zhang, T. Taliercio, P. Lefebvre, B. Gil, N. Grandjean, B. Damilano, and J. Massies, Appl. Phys. Lett. **80**, 428 (2002).
[11] A. K. Viswanath, J. I. Lee, S. Yu, D. Kim, Y. Choi, and C.-H. Hong, J. Appl. Phys. **84**, 3848 (1998).
[12] B. Monemar, P. P. Paskov, J. P. Bergman, A. A. Toropov, T. V. Shubina, T. Malinauskas, and A. Usui, Phys. Status Solidi B **245**, 1723 (2008).
[13] F. Stokker-Cheregi *et al.*, Phys. Rev. B **79**, 245316 (2009).
[14] F. Stokker Cheregi, A. Vinattieri, E. Feltin, D. Simeonov, J.-F. Carlin, R. Butté, N. Grandjean, and M. Gurioli, Phys. Rev. B **77**, 125342 (2008).
[15] X. B. Zhang, T. Taliercio, S. Kalliakos, and P. Lefebvre, J. Phys.: Condens. Matter **13**, 7053 (2001).
[16] M. Wojdak, A. Wysmołek, K. Pakuła, and J. Baranowski, Phys. Status Solidi B **216**, 95 (1999).
[17] D. Y. Song, M. Basavaraj, S. A. Nikishin, M. Holtz, V. Soukhoveev, A. Usikov, and V. Dmitriev, J. Appl. Phys. **100**, 113504 (2006).
[18] S. J. Xu, W. Liu, and M. F. Li, Appl. Phys. Lett. **77**, 3376 (2000).
[19] S. J. Xu, G. Q. Li, S.-J. Xiong, and C. M. Che, J. Appl. Phys. **99**, 073508 (2006).
[20] I. A. Buyanova *et al.*, Solid State Commun. **105**, 497 (1998).
[21] W. Liu, M. F. Li, S. J. Xu, K. Uchida, and K. Matsumoto, Semicond. Sci. Technol. **13**, 769 (1998).
[22] M. G. Tkachman, T. V. Shubina, V. N. Jmerik, S. V. Ivanov, P. S. Kopév, T. Paskova, and B. Monemar, Semiconductors **37**, 532 (2003).
[23] S. J. Xu, G. Q. Li, S. J. Xiong, S. Y. Tong, C. M. Che, W. Liu, and M. F. Li, J. Chem. Phys. **122**, 244712 (2005).
[24] D. Kovalev, B. Averboukh, D. Volm, B. K. Meyer, H. Amano, and I. Akasaki, Phys. Rev. B **54**, 2518 (1996).
[25] I. A. Buyanova, J. P. Bergman, B. Monemar, H. Amano, and I. Akasaki, Mater. Sci. Eng., B **50**, 130 (1997).
[26] B. Segall and G. D. Mahan, Phys. Rev. **171**, 935 (1968).
[27] S. Permagorov, *Excitons* (North-Holland, Amsterdam, 1982).
[28] B. Gil and O. Briot, Phys. Rev. B **55**, 2530 (1997).
[29] V. Y. Davydov, Y. E. Kitaev, I. N. Goncharuk, A. N. Smirnov, J. Graul, O. Semchinova, D. Uffmann, M. B. Smirnov, A. P. Mirgorodsky, and R. A. Evarestov, Phys. Rev. B **58**, 12899 (1998).
[30] T. Ruf, J. Serrano, M. Cardona, P. Pavone, M. Pabst, M. Krisch, M. D'Astuto, T. Suski, I. Grzegory, and M. Leszczynski, Phys. Rev. Lett. **86**, 906 (2001).
[31] J. M. Zhang, T. Ruf, M. Cardona, O. Ambacher, M. Stutzmann, J.-M. Wagner, and F. Bechstedt, Phys. Rev. B **56**, 14399 (1997).
[32] L. Siozade, J. Leymarie, P. Disseix, A. Vasson, M. Mihailovic, N. Grandjean, M. Leroux, and J. Massies, Solid State Commun. **115**, 575 (2000).
[33] E. Namvar and M. Fattahi, J. Lumin. **128**, 155 (2008).
[34] M. A. Reshchikov, G.-C. Yi, and B. W. Wessels, Phys. Rev. B **59**, 13176 (1999).
[35] M. Gurioli, A. Vinattieri, J. Martinez-Pastor, and M. Colocci, Phys. Rev. B **50**, 11817 (1994).
[36] Most likely, the poor thermal conductivity of the sapphire substrate prevents reaching T_{eff} at the lower temperatures, our cryostat being a cold finger type. We do not consider this as a fundamental issue, once the presence of thermalization has been proved.
[37] S. Shokhovets, O. Ambacher, and G. Gobsch, Phys. Rev. B **76**, 125203 (2007).
[38] S. Shokhovets, G. Gobsch, and O. Ambacher, Appl. Phys. Lett. **86**, 161908 (2005).
[39] P. A. Shields, R. J. Nicholas, F. M. Peeters, B. Beaumont, and P. Gibart, Phys. Rev. B **64**, 081203 (2001).
[40] J. D. Albrecht, P. P. Ruden, and T. L. Reinecke, J. Appl. Phys. **92**, 3803 (2002).